

# Structures of manganese polysulfides: mass-selected photodissociation and density functional calculations†

Yu-Chao Zhao, Jinyun Yuan, Zeng-Guang Zhang, Hong-Guang Xu and Weijun Zheng\*

Received 7th September 2010, Accepted 8th December 2010

DOI: 10.1039/c0dt01179g

Manganese polysulfide cations,  $\text{MnS}_x^+$  ( $x = 1-10$ ), were studied with mass-selected photodissociation experiments and density functional calculations. We found that  $\text{MnS}^+$ ,  $\text{MnS}_2^+$  and  $\text{MnS}_3^+$  undergo dissociation at 355 nm by loss of S,  $\text{S}_2$  and  $\text{S}_3$ , respectively. The dissociation of larger clusters is relatively complex because of the existence of multiple isomers and multiple dissociation channels. The geometric structures of the low-lying isomers found by theoretical calculations are consistent with the dissociation channels observed in the experiments. The dissociation of  $\text{MnS}_x^+$  clusters occurs mainly by breaking of the Mn–S bonds since they are weaker than the S–S bonds.

## 1. Introduction

Transition-metal sulfides have been studied by many research groups in the past decades as they have important applications in superconductors,<sup>1,2</sup> biochemical systems,<sup>3</sup> and catalytic processes.<sup>4</sup> Dance and co-workers generated many transition-metal sulfides using the laser ablation method and analyzed them by Fourier-transform ion cyclotron resonance (FTICR) mass spectrometry.<sup>5-11</sup> Liang *et al.* investigated the sulfides of group 4–6, 8 and 10 transition metals using matrix-isolation infrared spectroscopy and DFT calculations.<sup>12-16</sup> Nakajima and co-workers conducted anion photoelectron spectroscopy studies of iron–sulfur and manganese–sulfur clusters.<sup>17-19</sup> Gemming *et al.* investigated the structures of molybdenum sulfide clusters.<sup>20</sup> Gao and co-workers studied the photodissociation of tantalum–sulfur,<sup>21</sup> iron–sulfur,<sup>22</sup> cobalt–sulfur cluster ions,<sup>23</sup> and many other transition-metal sulfides.<sup>24-30</sup> Kretzschmar *et al.* investigated the thermochemistry and reactivity of a number of transition-metal sulfides (M–V, Mo, Sc, Ti) in the gas phase.<sup>31,32</sup> Bernstein and co-workers studied the formation and stability of neutral vanadium–sulfide clusters using multiphoton ionization.<sup>33</sup>

Among the transition-metal sulfides, transition-metal polysulfides belong to a special category showing novel structural and reactive properties.<sup>34,35</sup> They have potential applications in chemical industrial catalysis<sup>36</sup> and in battery cathodes,<sup>37</sup> and thus have attracted particular attention. Photodissociation, collision-induced dissociation and ion–molecule reaction experiments were used to study  $\text{FeS}_{1-6}^+$  clusters.<sup>38</sup>  $\text{FeS}_{1-6}^-$  cluster anions

were studied with photoelectron spectroscopy.<sup>39</sup>  $\text{FeS}_n^+$  ( $n = 2-8$ ),  $\text{TaS}_n^+$  ( $n = 4-10$ ), and  $\text{CoS}_n^+$  ( $n = 4, 6$ ) were explored by photodissociation experiments.<sup>21-23</sup> The formation and structures of the polysulfides of many other transition metals (except Tc) were investigated using laser ablation and FTICR mass spectrometry.<sup>9,40</sup> As for manganese, its sulfides and polysulfides were generated in the gas phase by laser ablation of solid MnS and were investigated using collision-induced dissociation method and density functional calculations.<sup>11,41</sup> Nevertheless, our knowledge about the properties of manganese polysulfides is not conclusive. To further explore the structural properties of manganese polysulfides, here we investigated  $\text{MnS}_n^+$  ( $n = 1-10$ ) by mass-selected photodissociation experiments and density functional calculations.

## 2. Experimental and theoretical methods

The experiments were conducted on a home-built reflectron time-of-flight mass spectrometer (RTOF-MS) which has been described elsewhere.<sup>42</sup> Briefly, the manganese–sulfur clusters were generated in the source chamber by ablating a rotating and translating Mn/S mixture disk target (13 mm diameter, Mn/S molar ratio 1 : 2) using the second harmonic output (532 nm, 10 mJ pulse<sup>-1</sup>, 5 Hz) of an Nd:YAG laser. The resulting plasma was cooled with argon carrier gas expanded through a pulsed valve (General Valve Series 9) at 3–5 atm backing pressure. The produced Mn/S cluster ions were mass-analyzed with the RTOF-MS. A selection–deceleration–dissociation–reacceleration method was used in the dissociation experiments. The  $\text{MnS}_n^+$  ( $n = 1-10$ ) cluster ions were mass-selected with a mass-gate at the first space focus point of the RTOF-MS, decelerated with an electric field, and dissociated with a second Nd:YAG laser (Continuum Surelite II-10) at 532 (69 mJ pulse<sup>-1</sup>, 5 ns) and 355 nm (21 mJ pulse<sup>-1</sup>, 5 ns) wavelengths without focusing the laser beam. The fragment ions and surviving

Beijing National Laboratory for Molecular Sciences, State Key Laboratory of Molecular Reaction Dynamics, Institute of Chemistry, Chinese Academy of Sciences, Beijing, 100190, China. E-mail: zhengwj@iccas.ac.cn; Fax: +86 10 62563167; Tel: +86 10 62635054

† Electronic supplementary information (ESI) available. See DOI: 10.1039/c0dt01179g

parent ions were then reaccelerated and detected by the MCP (microchannel plate) detector of the RTOF-MS. The ion signals were amplified with a broadband amplifier and recorded with a 100 MHz digital card, and were then collected in a laboratory computer with home-made software.

*Ab initio* calculations were performed using the Gaussian 03 package.<sup>43</sup> The geometric optimizations were conducted using Becke's three parameters hybrid functional<sup>44</sup> and the Lee, Yang and Parr correlation functional<sup>45,46</sup> (B3LYP) in conjunction with the 6-31g(d) basis set. The single-point energies of all optimized structures were calculated at the B3LYP theory level in conjunction with the mixed basis sets (S: aug-cc-pvqz; Mn: 6-311++G(3df)). The frequency analysis and zero-point energy corrections (ZPE) were also implemented at the same method as that of structural optimizations. It has been verified that all of the optimized structures have no imaginary frequencies. We have tested the theoretical method by calculating the bond dissociation energies (BDEs) of  $\text{MnS}^+$  and  $\text{S}_2$  as well as the ionization energy of  $\text{S}_2$ . Our calculations show that the BDEs of  $\text{MnS}^+$  and  $\text{S}_2$  are 2.48 and 4.38 eV respectively, in agreement with the experimental values ( $2.52 \pm 0.24$  eV for  $\text{MnS}^+$ ,<sup>47</sup> and  $4.41 \pm 0.13$  eV for  $\text{S}_2$ <sup>48</sup>) in the literature. The calculated ionization energy of  $\text{S}_2$  is about 9.56 eV, which is also close to the experimental value of  $9.36 \pm 0.02$  eV.<sup>49</sup> Thus, the comparison of theoretical calculations and experimental values demonstrated that the method chosen here is suitable for Mn–S clusters.

### 3. Experimental results

Fig. 1 shows a typical and reproducible mass spectrum of  $\text{Mn}_x\text{S}_y^+$  cluster ions generated in the experiments. There are three series of clusters,  $\text{S}_x^+$  ( $x = 2-13$ ),  $\text{MnS}_x^+$  ( $x = 0-14$ ), and  $\text{Mn}_2\text{S}_x^+$  ( $x = 0-12$ ). In these three series, the predominant mass peaks in the spectrum are those of  $\text{S}_x^+$  and  $\text{MnS}_x^+$ . The mass peaks of the  $\text{Mn}_2\text{S}_x^+$  clusters are weaker than those of  $\text{S}_x^+$  and  $\text{MnS}_x^+$ .

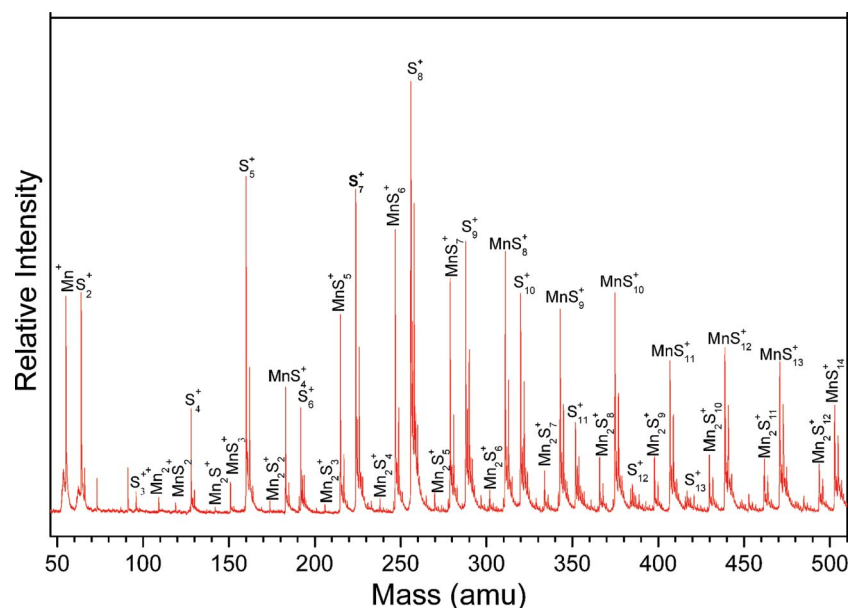


Fig. 1 Mass spectrum of  $\text{Mn}_x\text{S}_y^+$  cluster ions.

Fig. 2 and Fig. 3 show the photodissociation mass spectra of the  $\text{MnS}_x^+$  ( $x = 1-10$ ) clusters at 355 and 532 nm wavelengths, respectively. Generally, the efficiency of photodissociation at 532 nm is much lower than that at 355 nm. No dissociation fragments have been observed for  $\text{MnS}_{2,3,9,10}^+$  at 532 nm.

$\text{MnS}^+$ ,  $\text{MnS}_2^+$  and  $\text{MnS}_3^+$  undergo dissociation at 355 nm by loss of S,  $\text{S}_2$  and  $\text{S}_3$ , respectively. They all produced  $\text{Mn}^+$  fragment ions but with very low efficiency. At 532 nm,  $\text{Mn}^+$  fragment ion was detected for  $\text{MnS}^+$  but no fragment ion has been detected for  $\text{MnS}_2^+$  and  $\text{MnS}_3^+$ .

$\text{MnS}_4^+$ ,  $\text{MnS}_6^+$  and  $\text{MnS}_8^+$  undergo dissociation at 355 nm by loss of  $\text{S}_2$  units until reaching the smallest fragment ion,  $\text{Mn}^+$ .  $\text{MnS}_5^+$  and  $\text{MnS}_7^+$  undergo dissociation at 355 nm by loss of  $\text{S}_2$  units until reaching the fragment ion,  $\text{MnS}_3^+$ , then the fragment ion  $\text{MnS}_3^+$  loses  $\text{S}_3$  to generate  $\text{Mn}^+$ . A very tiny amount of  $\text{MnS}^+$  and  $\text{MnS}_2^+$  fragment ions for  $\text{MnS}_7^+$  as well as  $\text{MnS}^+$  fragment ions for  $\text{MnS}_6^+$  are barely distinguishable. At 532 nm, the dissociation of  $\text{MnS}_{4-8}^+$  still shows the same trend except that the  $\text{Mn}^+$  fragment ion was not detected for  $\text{MnS}_{5-8}^+$ . The smallest fragment ion at 532 nm for  $\text{MnS}_6^+$  and  $\text{MnS}_8^+$  is  $\text{MnS}_2^+$  instead of  $\text{Mn}^+$ . The smallest fragment ion at 532 nm for  $\text{MnS}_5^+$  and  $\text{MnS}_7^+$  is  $\text{MnS}_3^+$  instead of  $\text{Mn}^+$ . These results are consistent with the low dissociation efficiency or non-dissociation of  $\text{MnS}_2^+$  and  $\text{MnS}_3^+$  at 532 nm.

The major fragment ions of  $\text{MnS}_9^+$  at 355 nm are  $\text{MnS}_5^+$ ,  $\text{MnS}_4^+$ ,  $\text{MnS}_3^+$  and  $\text{Mn}^+$  while the minor ones are  $\text{MnS}_2^+$  and  $\text{MnS}^+$ . More likely, the photodissociation of  $\text{MnS}_9^+$  occurs first by loss of an  $\text{S}_4$  or  $\text{S}_5$  unit. Then, the  $\text{MnS}_4^+$  and  $\text{MnS}_5^+$  fragments are further photodissociated to generate other fragment ions. However, it is worth noting that the sub-dissociation of  $\text{MnS}_4^+$  fragment of  $\text{MnS}_9^+$  might be different from that of the  $\text{MnS}_4^+$  parent ion, because the signal of the  $\text{MnS}_2^+$  fragment ion in the  $\text{MnS}_9^+$  spectrum is much lower than that in the  $\text{MnS}_4^+$  spectrum. Photodissociation of  $\text{MnS}_{10}^+$  produces  $\text{MnS}_6^+$ ,  $\text{MnS}_4^+$ ,  $\text{MnS}_2^+$  and  $\text{Mn}^+$  fragments. The photodissociation of  $\text{MnS}_{10}^+$  probably occurs by initial loss of an  $\text{S}_4$  unit.

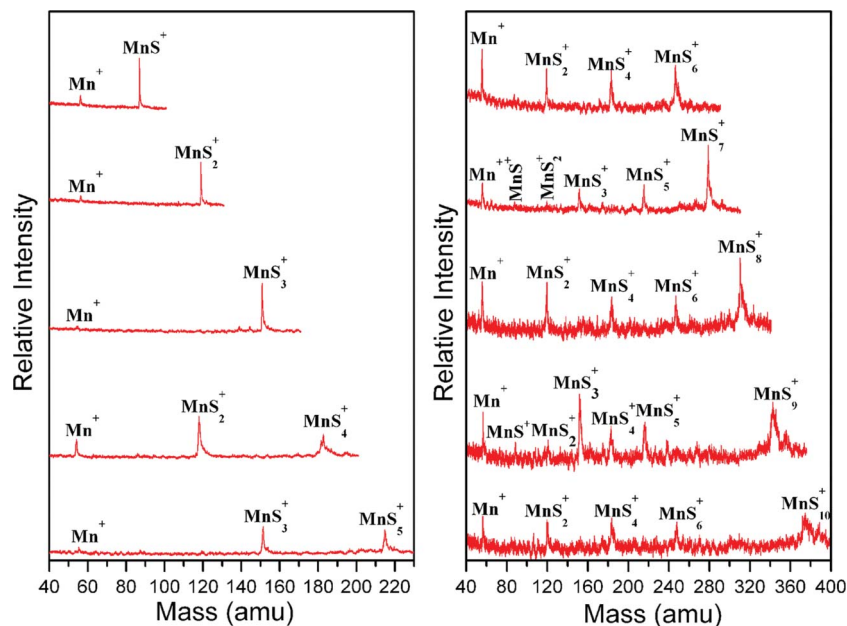


Fig. 2 Photodissociation mass spectra of  $\text{MnS}_y^+$  ( $y = 1-10$ ) clusters at 355 nm wavelength.

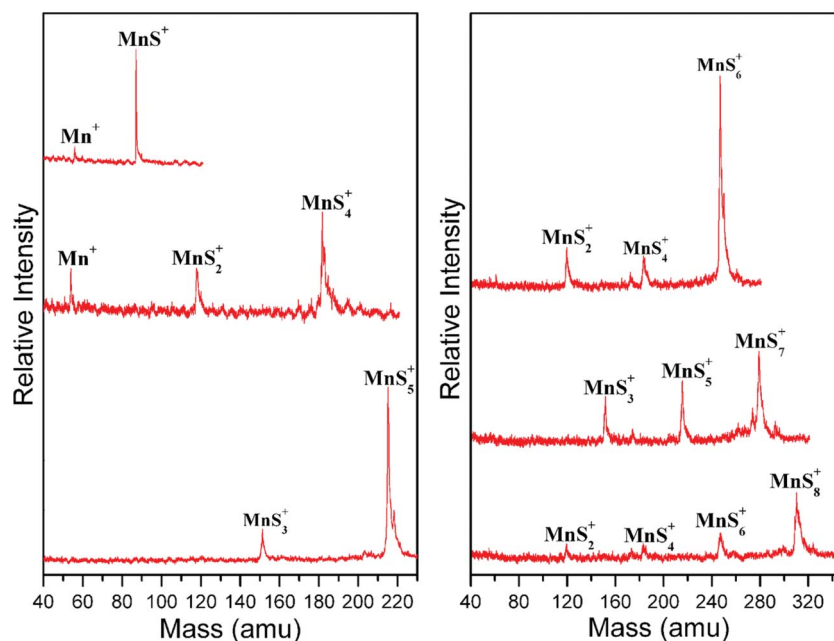


Fig. 3 Photodissociation mass spectra of  $\text{MnS}_y^+$  ( $y = 1-10$ ) clusters at 532 nm wavelength.

#### 4. Theoretical results and discussion

Fig. 4 shows the structures of the low-lying isomers of  $\text{MnS}_x^+$  ( $x = 1-8$ ) clusters with the most stable ones on the left.

##### $\text{MnS}^+$

The most stable structure of  $\text{MnS}^+$  is isomer 1A in the  $^5\text{S}_g$  state. Isomer 1B is in the  $^7\text{S}_g$  state, which is 0.33 eV higher than isomer 1A in energy. Our calculations show that the bond dissociation energy (BDE) of isomer 1A is 2.48 eV which is in agreement with the experimental value of 2.52 eV, and that of isomer 1B is 2.18 eV. A 355 nm photon is able to dissociate isomer 1A and 1B. A

532 nm photon can only dissociate isomer 1B. In our spectra, the relative intensity of the fragment ion  $\text{Mn}^+$  at 355 nm (Fig. 2) is higher than that at 532 nm (Fig. 3). We suggest that both isomers 1A and 1B exist in our experiment. The intensity of the fragment ion  $\text{Mn}^+$  at 355 nm probably is contributed by both isomers 1A and 1B, while that at 532 nm probably is contributed by isomer 1B only.

##### $\text{MnS}_2^+$

The most stable structure of  $\text{MnS}_2^+$  is isomer 2A in the  $^7\text{A}_2$  state. Isomers 2B and 2C are in  $^5\text{A}_2$  and  $^5\text{A}''$  states, respectively, which are

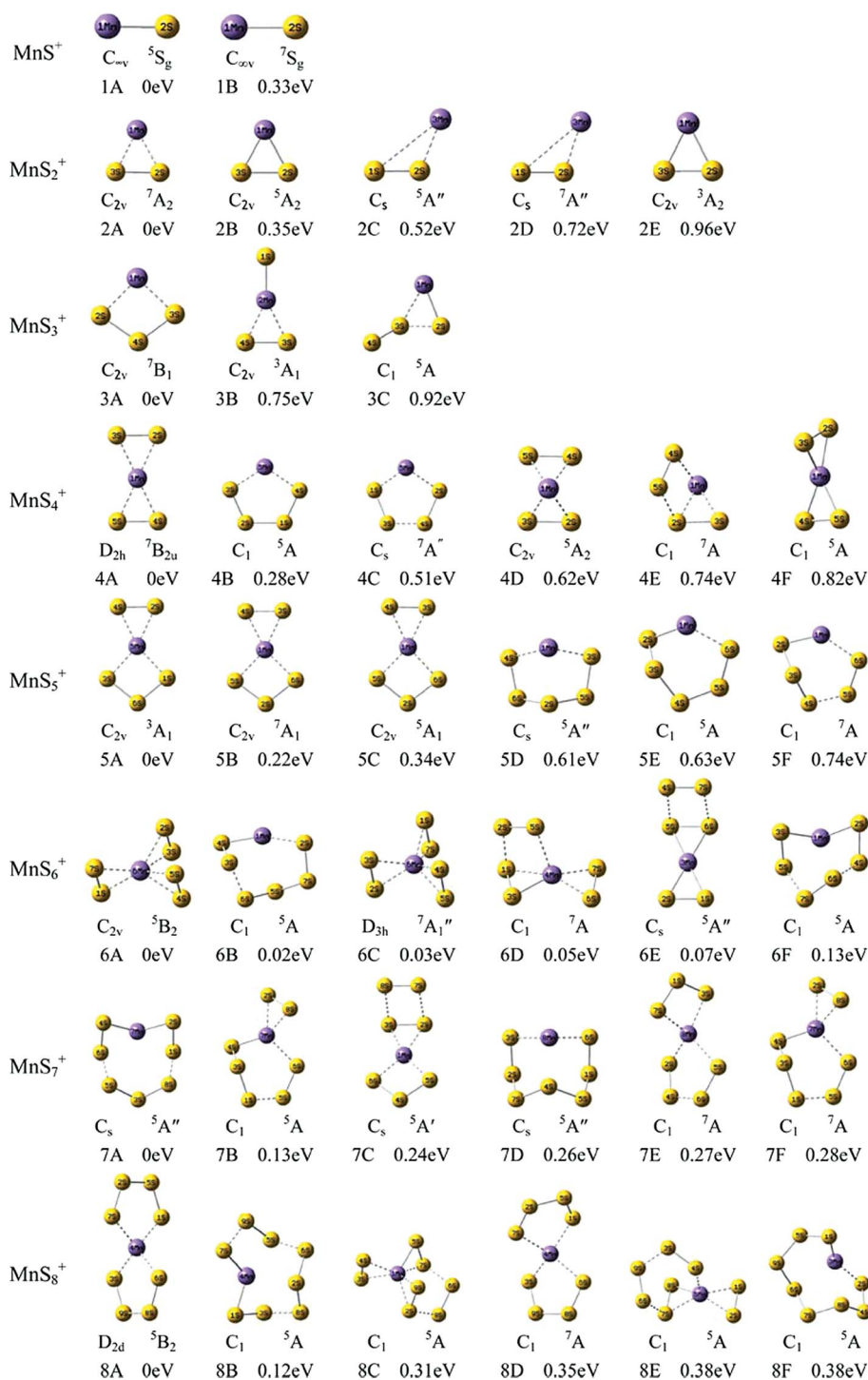


**Fig. 4** Structures of the low-lying isomers of MnS<sub>x</sub><sup>+</sup> (x = 1–8) clusters.

0.35 and 0.52 eV higher than isomer 2A in energy. Isomers 2D and 2E are higher than isomer 2A by 0.72 and 0.96 eV, respectively. All of them are of type Mn<sup>+</sup>–S<sub>2</sub>. That is in agreement with the loss of an S<sub>2</sub> unit in the dissociation experiment. Zhang *et al.* suggest that the MnS<sub>2</sub> neutral has two types of isomers, Mn–S<sub>2</sub> and S=Mn=S.<sup>50</sup> We found the S=Mn<sup>+</sup>=S linear structure is much more unstable than isomer 2A being higher in energy than isomer 2A by at least 1.7 eV. Since isomers 2C, 2D and 2E are much higher in energy, they are unlikely to be populated in our experiments,

and isomers 2A and 2B are likely to be the major products in our experiments.

### MnS<sub>3</sub><sup>+</sup>

The most stable structure of MnS<sub>3</sub><sup>+</sup> is isomer 3A in the <sup>7</sup>A<sub>2</sub> state. Our calculation shows that the BDE of 3A is 2.70 eV. It can be only dissociated at the 355 nm wavelength in accordance with the dissociation experiments. We suggest that isomer 3A exists in our

experiment. Isomers 3B and 3C would undergo dissociation by loss of  $S_2$  to produce  $MnS^+$  fragment ion. However, the  $MnS^+$  fragment has not been observed in our experiments. Also, the isomers 3B and 3C are less stable than isomer 3A since their energies are much higher than that of isomer 3A. Thus, isomers 3B and 3C probably are not observed in the experiments.

### $MnS_4^+$

The most stable structure of  $MnS_4^+$  is isomer 4A in the  ${}^7B_{2u}$  state. We found that the BDE value for loss of the first  $S_2$  is 2.08 eV and for the second  $S_2$  is 1.70 eV. Thus, both 355 and 532 nm photons are able to dissociate isomer 4A to produce  $MnS_2^+$  and  $Mn^+$  fragment ions. That is in agreement with our experimental observation. We suggest that isomer 4A is present in our experiment. Isomer 4B is in the  ${}^5A$  state which is 0.28 eV higher than isomer 4A in energy. Our calculations show that it takes about 3.07 eV to dissociate isomer 4B into  $Mn^+$  and  $S_4$ . Thus, a 355 nm photon is able to dissociate isomer 4B to generate the  $Mn^+$  fragment, but a 532 nm photon cannot. Since the energy of isomer 4B is only 0.28 eV higher than isomer 4A, we suspect that it might also be present in our experiments.

### $MnS_5^+$

The most stable structure of  $MnS_5^+$  is isomer 5A in the  ${}^3A_1$  state. Isomers 5B and 5C are in  ${}^7A_1$  and  ${}^5A_1$  states respectively, whose structures are analogous to that of isomer 5A. They are 0.22 and 0.34 eV higher than isomer 5A in energy, respectively. The energy of isomers 5D, 5E and 5F are much higher than isomer 5A and probably are not observed in the experiments. For isomers 5A, 5B and 5C, the BDE of the loss of  $S_2$  is lower than that of the loss of  $S_3$ . Thus, the most probable dissociation pattern is that isomers 5A, 5B and 5C first undergo dissociation by the loss of  $S_2$  to produce the  $MnS_3^+$  fragment, and then the  $MnS_3^+$  fragments undergo dissociation by loss of  $S_3$  to produce  $Mn^+$ . This is in agreement with the observation of  $MnS_3^+$  and  $Mn^+$  in the dissociation experiment of  $MnS_5^+$  at 355 nm. As shown earlier,  $MnS_3^+$  cannot be dissociated by a 532 nm photon, thus, no  $Mn^+$  was produced in the dissociation of  $MnS_5^+$  at 532 nm.

### $MnS_6^+$

The low-lying isomers of  $MnS_6^+$  are very close in energy and are all probably present in our experiments. Isomers 6A and 6C have similar structures but are in different electronic states. Both of them can undergo dissociation by sequential loss of  $S_2$  units to produce  $MnS_4^+$ ,  $MnS_2^+$  and  $Mn^+$  fragments. Our calculations show that isomers 6B, 6D, 6E and 6F all can undergo dissociation by sequential loss of  $S_2$  units. Loss of  $S_4$  is also possible for isomer 6E. These are consistent with the observation of  $MnS_4^+$ ,  $MnS_2^+$  and  $Mn^+$  fragments at 355 nm in our experiments. Isomer 6F probably can also lose  $S_6$  to generate  $Mn^+$  directly at 355 nm. No  $Mn^+$  fragment has been detected at 532 nm probably because the energy of 532 nm photons is too low to generate  $Mn^+$  directly from isomer 6F, or to generate  $Mn^+$  indirectly from the  $MnS_2^+$  fragment ion.

### $MnS_7^+$

Isomers 7A and 7D photodissociated by 355 nm photons can lose  $S_7$  to produce the  $Mn^+$  fragment directly. Isomers 7B and 7F have similar structures but are in different electronic states and they all can generate the  $MnS_5^+$  fragment by loss of  $S_2$ . Isomer 7C can be dissociated to produce  $MnS_5^+$  and  $MnS_3^+$  fragments by loss of  $S_2$  or  $S_4$  units. Isomer 7E probably has the same photodissociation pattern as isomer 7C since their geometric structures are similar, that is, they consist of  $S_3$  and  $S_4$  units.

### $MnS_8^+$

Our calculations show that isomers 8A and 8D can be dissociated by loss of one  $S_4$  unit or by loss of  $S_2$  units. Isomers 8C and 8E can be dissociated by loss of four  $S_2$  units sequentially. Thus, they are able to produce  $MnS_6^+$ ,  $MnS_4^+$ ,  $MnS_2^+$  and  $Mn^+$  fragment ions at 355 nm. Isomers 8B and 8F might be able to generate a  $Mn^+$  fragment by loss of  $S_8$  at 355 nm. No  $Mn^+$  fragment has been observed at 532 nm because a 532 nm photon is not able to initiate loss of  $S_8$  from isomers 8B and 8F or loss of  $S_2$  from the  $MnS_2^+$  fragment ion. The calculated structures of  $MnS_8^+$  are consistent with dissociation products detected in the experiments.

### $MnS_9^+$ and $MnS_{10}^+$

As shown in the experiments (Fig. 2), the first step of photodissociation of  $MnS_9^+$  is dissociation of the  $S_4$  or  $S_5$  unit to produce the fragment ions  $MnS_5^+$  or  $MnS_4^+$ , respectively. Then, the fragment ion  $MnS_5^+$  can be photodissociated to produce the fragment ions  $MnS_3^+$  and  $MnS_2^+$  and finally the fragment ion  $MnS_3^+$  may be photodissociated to produce the ion  $Mn^+$ , and the fragment ion  $MnS_2^+$  may be also photodissociated to generate the ions  $MnS^+$  and  $Mn^+$ , in which the yield of  $Mn^+$  is larger than that of  $MnS^+$ . According to the photodissociation experimental results, it might be possible that  $MnS_9^+$  is composed of  $S_4$  and  $MnS_5^+$  units and the structural unit  $MnS_5^+$  might consist of  $S_2$  and  $MnS_3^+$ .  $MnS_{10}^+$  is firstly photodissociated by loss of an  $S_4$  unit to produce the  $MnS_6^+$  fragment ion at 355 nm. Subsequently, the daughter ion  $MnS_6^+$  can be further photodissociated to produce the other fragment ions such as  $MnS_4^+$ ,  $MnS_2^+$  and  $Mn^+$ . Therefore, we speculate that  $MnS_{10}^+$  would be composed of  $S_4$  and  $MnS_6^+$  units. Multiple isomers probably also exist for  $MnS_9^+$  and  $MnS_{10}^+$ .

Dance and co-workers calculated the molecular structures of  $Mn_xS_y$  neutrals.<sup>41</sup> They found the most stable structure of  $MnS_2$  neutral is linear and that of  $MnS_3$  neutral has a triangular structure formed by the three S atoms and the Mn atom is at the center of the triangle. Our calculations show that the linear structure of  $MnS_2$  neutral is unstable for  $MnS_2^+$ . The planar triangular isomer found for  $MnS_3$  neutral is unstable for  $MnS_3^+$ . Gao and co-workers reported the photodissociation of  $TaS_n^+$ ,  $FeS_n^+$  and  $CoS_n^+$  clusters using 248 nm photons.<sup>21–23</sup> In the photodissociation of  $TaS_n^+$  clusters, the main dissociation channel is the loss of  $S_2$  or  $S_4$ , however, the loss of S can also occur for  $TaS_4^+$ . The channels for loss of a sulfur atom were also observed for  $FeS_2^+$ ,  $FeS_3^+$ ,  $FeS_4^+$  and  $FeS_5^+$ . The dissociation channel of  $CoS_6^+$  is loss of  $S_4$ , while that of  $CoS_4^+$  is loss of  $S_2$ . Both the dissociations of  $CoS_4^+$  and  $CoS_6^+$  are of very low efficiency. In our experiments of  $MnS_x^+$  clusters, no dissociation channel for loss of S atom has been observed except for  $MnS^+$ . The dissociations of  $MnS_4^+$ ,  $MnS_6^+$  and other

larger clusters are much more efficient than those of  $\text{TaS}_n^+$ ,  $\text{FeS}_n^+$  and  $\text{CoS}_n^+$  clusters. The intensities of the fragment ions of  $\text{MnS}_x^+$  clusters at 355 nm are close to or higher than that of the remaining parent ions, which means the dissociation ratios are higher than 50%. For  $\text{MnS}_x^+$  with an even number of sulfur atoms, the main dissociation channel is the loss of  $\text{S}_2$  or  $\text{S}_4$ . For  $\text{MnS}_x^+$  with an odd number of sulfur atoms, the main dissociation channel is the loss of  $\text{S}_2$  units followed by loss of  $\text{S}_3$ . For the larger clusters, such as  $\text{MnS}_9^+$  and  $\text{MnS}_{10}^+$ , the loss of  $\text{S}_4$  can also happen.

As reported in the literature, the BDE of  $\text{MnS}^+$  is  $2.52 \pm 0.24$  eV,<sup>47</sup> and that of  $\text{S}_2$  is  $4.41 \pm 0.13$  eV.<sup>48</sup> The S–S bonds are stronger than the Mn–S bonds. This implies that the dissociation of  $\text{MnS}_x^+$  clusters would occur mainly by breaking of the Mn–S bonds. That is consistent with what is observed in the dissociation experiments (Fig. 2 and 3). We found that for the most probable isomers of  $\text{MnS}_2^+$  and  $\text{MnS}_3^+$ , the coordination number of  $\text{Mn}^+$  is 2. For  $\text{MnS}_x^+$  ( $x = 4-8$ ) clusters, the coordination number of  $\text{Mn}^+$  can be 2, 4 or 6. Among them, the clusters have more inclination to form four-coordinated structures.

## 5. Conclusions

We studied the photodissociation of  $\text{MnS}_x^+$  ( $x = 1-10$ ) clusters and calculated the geometric structures of  $\text{MnS}_x^+$  ( $x = 1-8$ ) using density functional method. We found that  $\text{MnS}^+$ ,  $\text{MnS}_2^+$  and  $\text{MnS}_3^+$  undergo dissociation at 355 nm by loss of S,  $\text{S}_2$  and  $\text{S}_3$ , respectively. Dissociation of  $\text{MnS}_5^+$  and  $\text{MnS}_7^+$  at 355 nm first generated  $\text{MnS}_3^+$  by loss of  $\text{S}_2$  units, then generated  $\text{Mn}^+$  by loss of an  $\text{S}_3$  unit. The clusters with an even number of sulfur atoms, such as  $\text{MnS}_4^+$ ,  $\text{MnS}_6^+$  and  $\text{MnS}_8^+$ , undergo dissociation mainly by sequential loss of  $\text{S}_2$  or  $\text{S}_4$  units. Comparison of the experimental data and theoretical calculations suggests that the  $\text{MnS}_x^+$  clusters coexist as multiple isomers. The structures of the low-lying isomers of  $\text{MnS}_x^+$  clusters are characterized by addition of  $\text{S}_n$  ( $n \leq x$ ) units to the  $\text{Mn}^+$  ion. The  $\text{Mn}^+$  ion coordinates with the S atoms at the two ends of the  $\text{S}_n$  units to form  $(n + 1)$ -membered rings. The number of  $\text{S}_n$  units connecting to the  $\text{Mn}^+$  ion can be two, one or three, with more inclination towards two; hence, most of the isomers have double ring structures. The most stable isomer of  $\text{MnS}_8^+$  has a  $(\text{S}_4)\text{Mn}^+(\text{S}_4)$  style double five-membered ring structure.

## Acknowledgements

W. J. Z. acknowledges the Institute of Chemistry, Chinese Academy of Sciences for start-up funds. We are grateful to Professor Zhen Gao for valuable discussions. We thank the Supercomputing Center of Chinese Academy of Sciences for allowing us to use the ScGrid for theoretical calculations.

## References

- M. Kockerling, D. Johrendt and E. W. Finckh, *J. Am. Chem. Soc.*, 1998, **120**, 12297–12302.
- R. Chevrel, M. Hirrien and M. Sergent, *Polyhedron*, 1986, **5**, 87–94.
- B. Krebs and G. Henkel, *Angew. Chem., Int. Ed. Engl.*, 1991, **30**, 769–788.
- S. Harris and R. R. Chianelli, *J. Catal.*, 1984, **86**, 400–412.
- J. H. El Nakat, I. G. Dance, K. J. Fisher, D. Rice and G. D. Willett, *J. Am. Chem. Soc.*, 1991, **113**, 5141–5148.
- J. H. El Nakat, I. G. Dance, K. J. Fisher and G. D. Willett, *Inorg. Chem.*, 1991, **30**, 2957–2958.
- J. Elnakat, I. Dance, K. Fisher and G. Willet, *J. Chem. Soc., Chem. Commun.*, 1991, 746–748.
- J. El Nakat, K. J. Fisher, I. G. Dance and G. D. Willett, *Inorg. Chem.*, 1993, **32**, 1931–1940.
- I. G. Dance, K. J. Fisher and G. D. Willett, *Inorg. Chem.*, 1996, **35**, 4177–4184.
- K. Fisher, I. Dance, G. Willett and M. N. Yi, *J. Chem. Soc., Dalton Trans.*, 1996, 709–718.
- I. G. Dance, K. J. Fisher and G. D. Willett, *J. Chem. Soc., Dalton Trans.*, 1997, 2557–2561.
- B. Liang and L. Andrews, *J. Phys. Chem. A*, 2002, **106**, 6295–6301.
- B. Liang and L. Andrews, *J. Phys. Chem. A*, 2002, **106**, 3738–3743.
- B. Liang and L. Andrews, *J. Phys. Chem. A*, 2002, **106**, 6945–6951.
- B. Liang, X. Wang and L. Andrews, *J. Phys. Chem. A*, 2009, **113**, 5375–5384.
- B. Liang, X. Wang and L. Andrews, *J. Phys. Chem. A*, 2009, **113**, 3336–3343.
- A. Nakajima, T. Hayase, F. Hayakawa and K. Kaya, *Chem. Phys. Lett.*, 1997, **280**, 381–389.
- N. Zhang, T. Hayase, H. Kawamata, K. Nakao, A. Nakajima and K. Kaya, *J. Chem. Phys.*, 1996, **104**, 3413–3419.
- N. Zhang, H. Kawamata, A. Nakajima and K. Kaya, *J. Chem. Phys.*, 1996, **104**, 36–41.
- S. Gemming, G. Seifert, M. Götz, T. Fischer and G. Ganteför, *Phys. Status Solidi B*, 2010, **247**, 1069–1076.
- N. Zhang, Z. D. Yu, X. J. Wu, Z. Gao, Q. H. Zhu and F. N. Kong, *J. Chem. Soc., Faraday Trans.*, 1993, **89**, 1779–1782.
- Z. D. Yu, N. Zhang, X. J. Wu, Z. Gao, Q. H. Zhu and F. N. Kong, *J. Chem. Phys.*, 1993, **99**, 1765–1770.
- Y. Shi, N. Zhang, Z. Gao, F. A. Kong and Q. H. Zhu, *J. Chem. Phys.*, 1994, **101**, 9528–9533.
- S. F. Wang, J. K. Feng, M. Cui, M. F. Ge, C. C. Sun, Z. Gao and F. A. Kong, *Chem. J. Chin. Univ. Chin.*, 1999, **20**, 1447–1451.
- P. Liu, C. Y. Han, Z. Gao, F. A. Kong and Q. H. Zhu, *J. Phys. Chem. B*, 1999, **103**, 3337–3339.
- W. D. Cui, X. Zhao, B. X. Peng, Y. Shi, Z. Gao, Q. H. Zhu and F. A. Kong, *Acta Chin. Sin.*, 1999, **57**, 1179–1184.
- W. J. Wang, D. P. Hu, P. Liu, Z. Gao, F. A. Kong and Q. H. Zhu, *Acta Chin. Sin.*, 1998, **56**, 675–681.
- B. X. Peng, W. D. Cui, Z. D. Yu, Z. Gao, Q. H. Zhu and F. A. Kong, *Sci. Chin. Ser. B, Chem.*, 1997, **40**, 309–315.
- Y. Shi, Z. D. Yu, N. Zhang, Z. Gao, F. A. Kong and Q. H. Zhu, *J. Chin. Chem. Soc.*, 1995, **42**, 455–460.
- Z. D. Yu, N. Zhang, Z. Gao, F. A. Kong and Q. H. Zhu, *Acta Phys. Chin. Sin.*, 1994, **10**, 97–99.
- I. Kretzschmar, D. Schroder, H. Schwarz, C. Rue and P. B. Armentrout, *J. Phys. Chem. A*, 2000, **104**, 5046–5058.
- I. Kretzschmar, D. Schroder, H. Schwarz and P. B. Armentrout, *Int. J. Mass Spectrom.*, 2003, **228**, 439–456.
- S. G. He, Y. Xie, Y. Guo and E. R. Bernstein, *J. Chem. Phys.*, 2007, **126**, 194315.
- M. Draganjac and T. B. Rauchfuss, *Angew. Chem., Int. Ed. Engl.*, 1985, **24**, 742–757.
- T. B. Rauchfuss, *Inorg. Chem.*, 2004, **43**, 14–26.
- N. Takeda, N. Tokitoh and R. Okazaki, in *Elemental Sulfur and Sulfur-Rich Compounds II*, R. Stuedal, Springer, 2004, vol. 231, pp. 153–202.
- W. L. Bowden, L. H. Barnette and D. L. Demuth, *J. Electrochem. Soc.*, 1988, **135**, 1–6.
- T. J. Macmahon, T. C. Jackson and B. S. Freiser, *J. Am. Chem. Soc.*, 1989, **111**, 421–427.
- H. J. Zhai, B. Kiran and L.-S. Wang, *J. Phys. Chem. A*, 2003, **107**, 2821–2828.
- I. Dance, K. Fisher and G. Willett, *Angew. Chem., Int. Ed. Engl.*, 1995, **34**, 201–203.
- I. G. Dance and K. J. Fisher, *J. Chem. Soc., Dalton Trans.*, 1997, 2563–2575.
- Y. C. Zhao, Z. G. Zhang, J. Y. Yuan, H. G. Xu and W. J. Zheng, *Chin. J. Chem. Phys.*, 2009, **22**, 655–662.
- M. J. Frisch, G. W. Trucks, H. B. Schlegel, G. E. Scuseria, M. A. Robb, J. R. Cheeseman, J. A. Montgomery, Jr., T. Vreven, K. N. Kudin, J. C. Burant, J. M. Millam, S. S. Iyengar, G. Tomasi, V. Barone, B. Mennucci, M. Cossi, G. Scalmani, N. Rega, G. A. Petersson, H. Nakatsuji, M. Hada, M. Ehara, K. Toyota, R. Fukuda, J. Hasegawa, M. Ishida, T.

- 
- Nakajima, Y. Honda, O. Kitao, H. Nakai, M. Klene, X. Li, J. E. Knox, H. P. Hratchian, J. B. Cross, V. Bakken, C. Adamo, J. Jaramillo, R. Gomperts, R. E. Stratmann, O. Yazyev, A. J. Austin, R. Cammi, C. Pomelli, J. Ochterski, P. Y. Ayala, K. Morokuma, G. A. Voth, P. Salvador, J. J. Dannenberg, V. G. Zakrzewski, S. Dapprich, A. D. Daniels, M. C. Strain, O. Farkas, D. K. Malick, A. D. Rabuck, K. Raghavachari, J. B. Foresman, J. V. Ortiz, Q. Cui, A. G. Baboul, S. Clifford, J. Cioslowski, B. B. Stefanov, G. Liu, A. Liashenko, P. Piskorz, I. Komaromi, R. L. Martin, D. J. Fox, T. Keith, M. A. Al-Laham, C. Y. Peng, A. Nanayakkara, M. Challacombe, P. M. W. Gill, B. G. Johnson, W. Chen, M. W. Wong, C. Gonzalez and J. A. Pople, *GAUSSIAN 03*, Gaussian, Inc., Wallingford, CT, 2004.
- 44 A. D. Becke, *J. Chem. Phys.*, 1993, **98**, 5648–5652.  
45 C. Lee, W. Yang and R. G. Parr, *Phys. Rev. B*, 1988, **37**, 785.  
46 B. Miehlich, A. Savin, H. Stoll and H. Preuss, *Chem. Phys. Lett.*, 1989, **157**, 200–206.  
47 C. Rue, P. B. Armentrout, I. Kretzschmar, D. Schroder and H. Schwarz, *Int. J. Mass Spectrom.*, 2001, **210**, 283–301.  
48 P. Budininkas, R. K. Edwards and P. G. Wahlbeck, *J. Chem. Phys.*, 1968, **48**, 2859–2866.  
49 J. Berkowitz and C. Lifshitz, *J. Chem. Phys.*, 1968, **48**, 4346–4350.  
50 N. Zhang, H. Kawamata, A. Nakajima and K. Kaya, *J. Chem. Phys.*, 1996, **104**, 36–41.